Electronic Supplementary Information

Single- and Bi-exciton Character in Ligand-modified Silicon Nanoparticles Characterized *via* Single Particle Photon Statistics and Plasmonic Effects

Woong Young So, Sikandar Abbas, Qi Li, Rongchao Jin, and Linda A. Peteanu*
Department of Chemistry, Carnegie Mellon University, Pittsburgh, PA, USA 15213

*Email (L. A. Peteanu) peteanu@cmu.edu

List of Supplemental Figures:

Additional Supplementary Information:

Calculation of the average excited state population <N> of the CT state

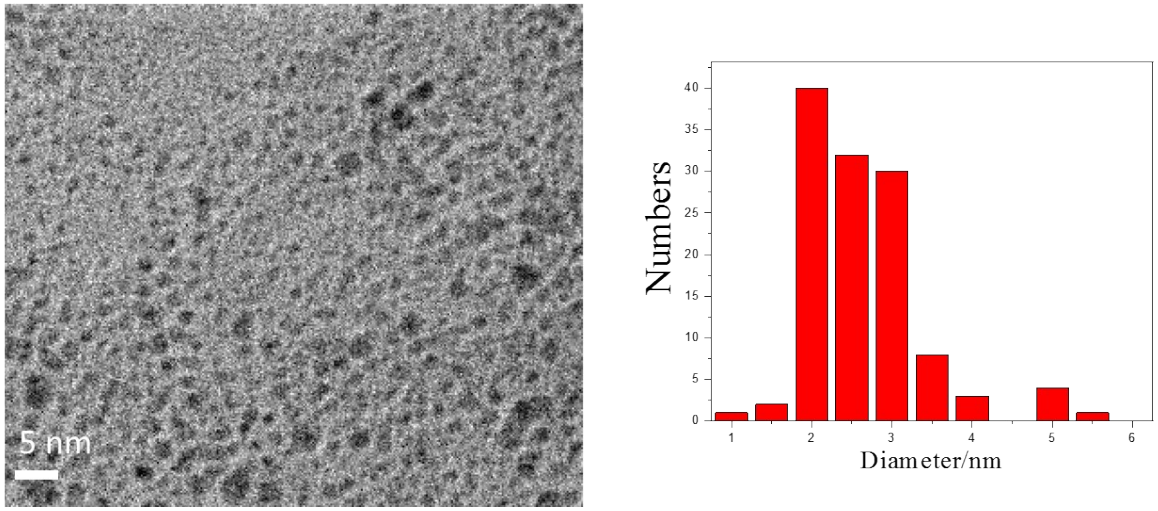

Figure S1. TEM analysis for Te-On Si NPs, 2.63 ± 0.28nm (N=316).

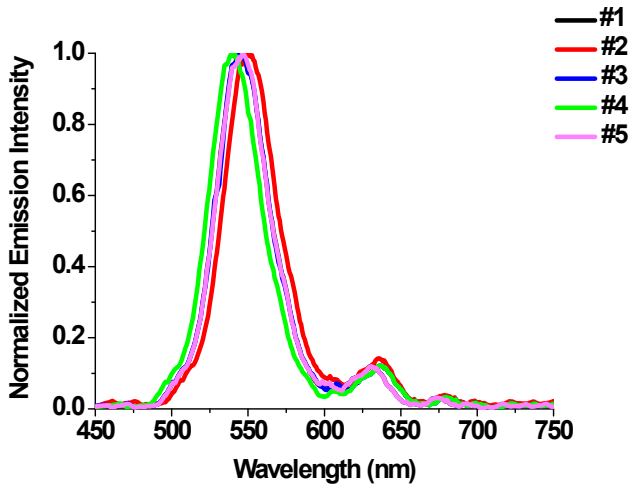

Figure S2. Replicates of Te-On Si NP single-particle dispersed emission spectra.

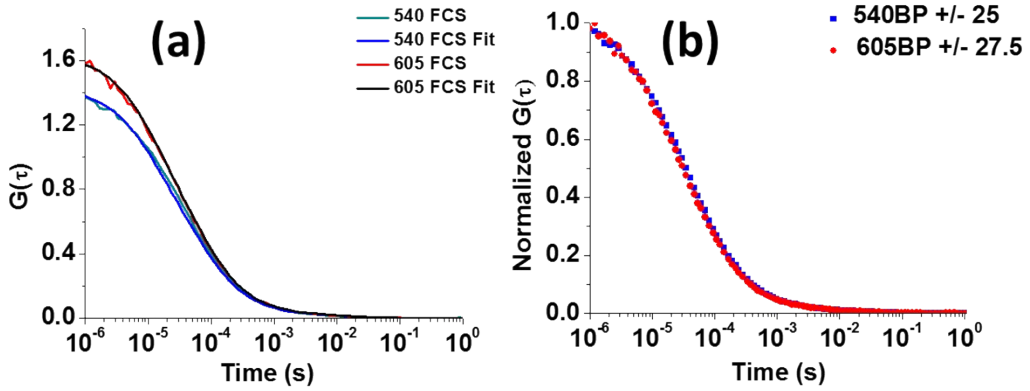

Figure S3. (a) FCS curves for Te-On Si NPs collected at 540nm and 605nm. (b) Normalized FCS curves collected at 540nm and 605nm.

FCS measures the diffusion of the fluorescent probes by monitoring the fluctuations of the photon intensities $I(t)$ in the focal volume. The FCS temporal correlation function, $G(\tau)$, is calculated by cross-correlating the photon intensities of the two detectors.[1] This quantity is defined as

$$G(\tau) = \frac{\langle \delta I(t) \delta I(t+\tau) \rangle}{\langle I(t) \rangle^2} \qquad (1)$$

where $\langle\ \rangle$ denotes an average over the entire trajectory, and $\delta I(t)$ is the deviation from the mean photon intensity at time t.

$$\delta I(t) = I(t) - \langle I(t) \rangle \qquad (2)$$

If the focal volume is assumed to have a three-dimensional Gaussian shape, the FCS curve is fitted to[2]

$$G(\tau) = \frac{1}{N} \sum_{i=1}^{n} a_i \left(1 + \frac{\tau}{\tau_{D_i}}\right)^{-1} \left(1 + \frac{1}{\omega^2} \frac{\tau}{\tau_{D_i}}\right)^{-\frac{1}{2}} \qquad (3)$$

where N is the average number of molecules in the focal volume, n is the number of species, a_i is the contribution of the *i*th species, τ_{D_i} is the characteristic residence time for the *i*th species, and $\omega(=z_0/r_0)$ characterizes the dimension of the focal volume with z_0 and r_0 being the axial and radial dimensions of the focal volume, respectively. Here *n* is taken to be unity. From Equation 3, the value of $G(\tau)$ at zero time is inversely proportional to number of emitters. Therefore, if the y-intercept in Figure S2 is equal to or larger than one then the concentration used in solution is in the single molecule regime. The value of $\omega = 0.2\mu m$ was used to fit the diffusion decays at 540nm and 605nm yielding values of $\tau_D = 0.0000481s$ at 540nm and $\tau_D = 0.0000486s$ at 605nm. The two curves yield a different number of emitters per focal volume, N, (0.71 at 540nm and 0.63 at 605nm) likely due to a higher degree of quenching of the red emission, which is consistent with the low yield in this wavelength region. The FCS curves collected at 540nm and 605nm are also overlaid (Figure S3b) to show the similarity in their diffusion decays (τ_D). This demonstrates the emission at both wavelengths arises from particles of similar size.

Additional information regarding the size of the diffusing particles was estimated by analysis of the FCS data. Based on the diffusion decay component (τ_D), the diffusion coefficient (D) could be obtained from the equation (Equation 4). Then, D at 540nm is determined to be 208μm^2/s while D at 605nm is determined to be 206μm^2/s.

$$D = \frac{\omega^2}{4\tau_D} \quad (4)$$

Then, the diffusion coefficient, D, allows the calculation of the size of the diffusing particles *via* the Stokes-Einstein relation.

$$r = \frac{k_B T}{6\pi\eta D} \quad (5)$$

where r is the hydrodynamic radius of particle, k_B is the Boltzmann constant, T is the temperature, and η is the viscosity of the solution (acetonitrile: 0.343mPa at $T = 298K$). Then, the size was

calculated to be 3.06nm at 540nm emission region and 3.09nm at 605nm emission region, proving that the two emission bands arise from particles having the same size. These values also compare well with the literature diameter size value of 2.8 nm for the Te-On Si nanoparticles.[3] From this we conclude that aggregation is not present under the conditions we used to perform these experiments in solution.

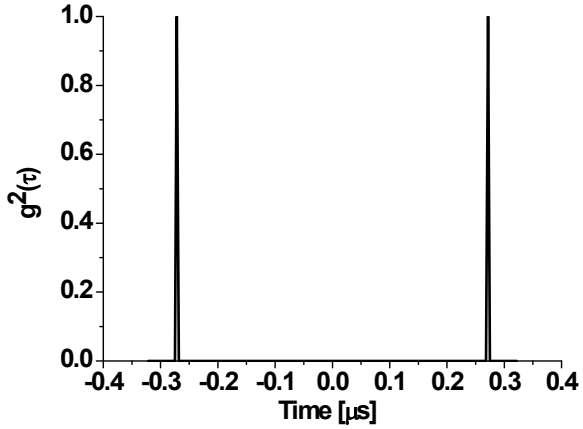

Figure S4. Normalized anti-bunching signal for a blank solution obtained with the laser operating at a 10MHz repetition rate (100ns between pulses).

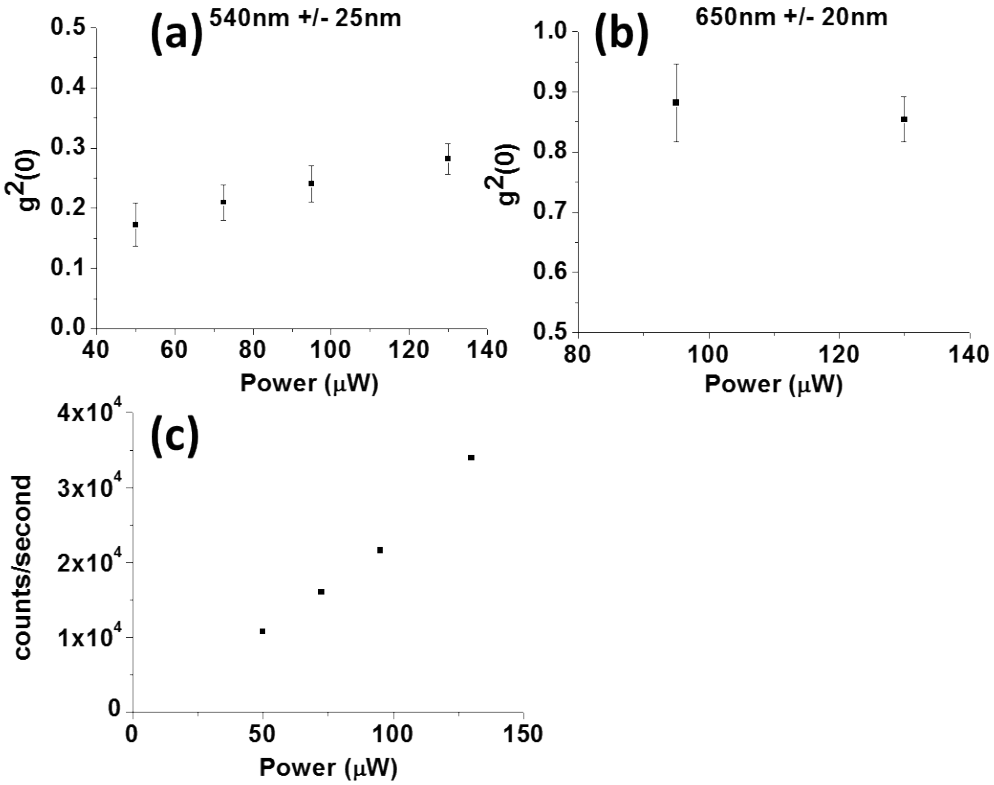

Figure S5. Power dependence of the value of $g^2(0)$ for Te-On Si NP at (a) the emission maximum (540nm) and (b) in the red region (650nm) showing sub-linear scaling. Unfortunately, the signal is too weak at 650nm to collect data at powers lower than 100μW. (c) Power dependence of the emission intensity of Te-On Si NPs at their emission maxima (540nm) showing approximately linear scaling.

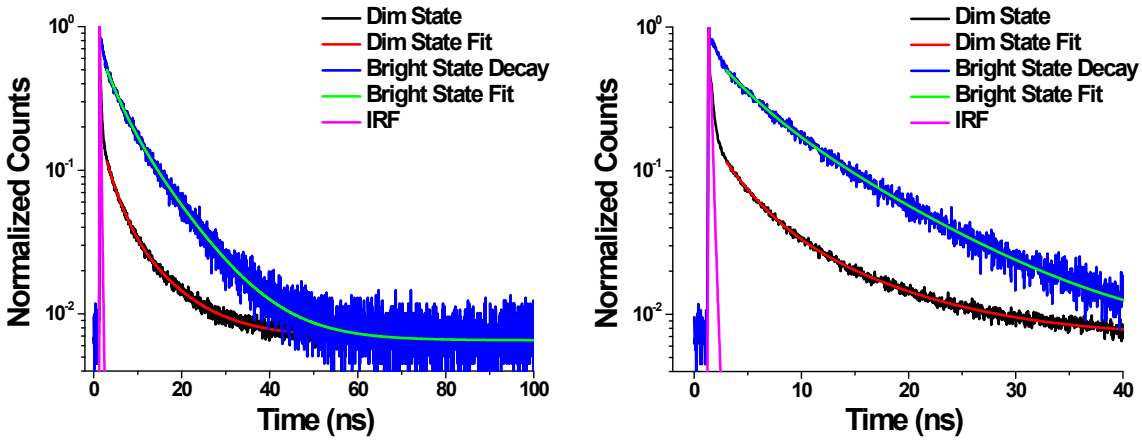

Figure S6. Normalized lifetime curves of Te-On Si NPs in PMMA for bright state (above 80 counts/10ms) and dim state (below 80 counts/10ms) with IRF at 540nm (see main text). On the right hand side, axis is expanded to make the IRF more visible.

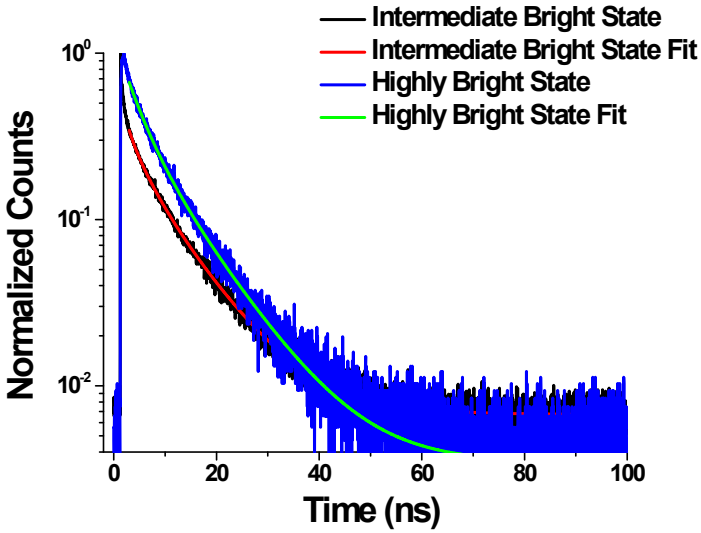

Figure S7. Comparison of the emission lifetime of Te-On Si NPs in PMMA for photon count rates corresponding to the intermediate bright state (300 counts/10ms – 80 counts/10ms) and the highly bright state (above 300 counts/10ms) at 540nm (see main text). Curves are normalized.

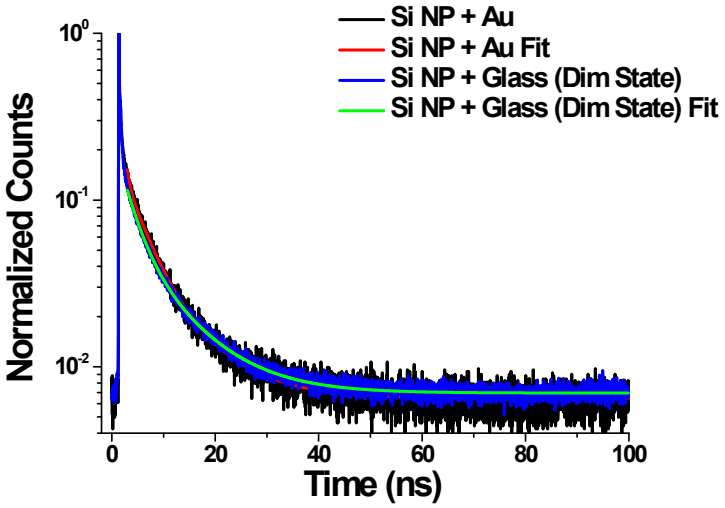

Figure S8. Comparison of the decay of the total emission of the Si NPs on Au at 540nm and that of the dim state (below 80 counts/10ms) on glass (see main text).

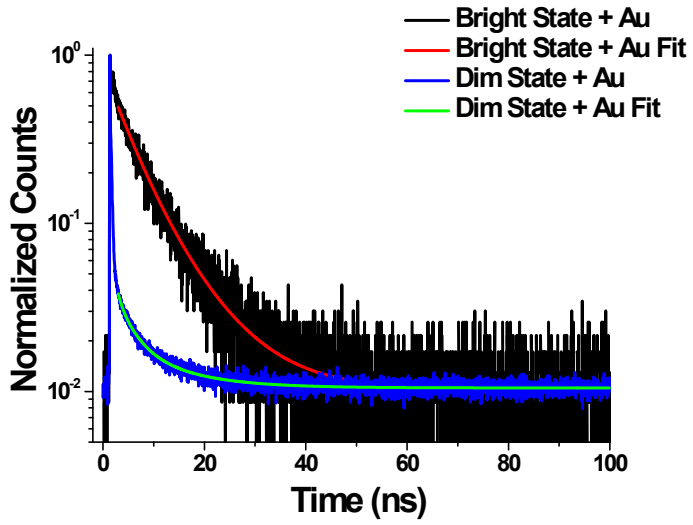

Figure S9. Comparison of the emission lifetime of Te-On Si NPs in PMMA/Au film for photon count rates corresponding to the bright state (above 80 counts/10ms) and the dim state (below 80 counts/10ms) at 540nm (see main text). Curves are normalized.

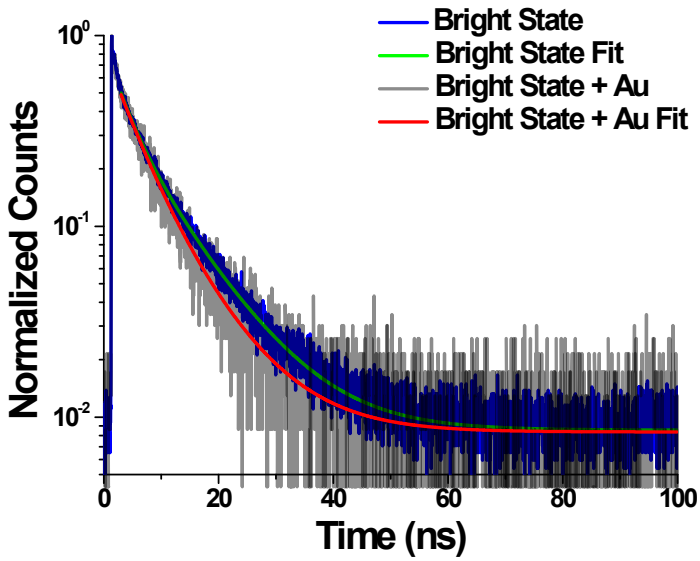

Figure S10. Comparison of the lifetime of the bright state emission of Si NPs on an uncoated glass substrate with that on Au collected at 540nm. The peak counts of the bright state are 800 counts on glass and 230 counts on gold. Curves are normalized.

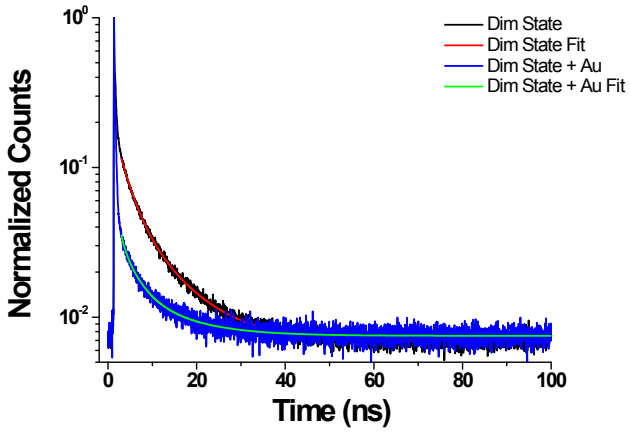

Figure S11. Comparison of the lifetime of the dim state emission of Si NPs on an uncoated glass substrate with that on Au collected at 540nm.

Calculation of the average excited state population <N> of the CT state

Note that this calculation is for <N> uses the parameters (absorption cross section, *ect.*) of the CT state. For pulsed excitation, <N> is given by

$$< N >= \frac{ln2P\sigma_{abs}}{E_p \Gamma \pi r^2}$$ where P is the average laser power, r is the radius of the focused laser beam, Γ is the laser repetition rate, E_p is the energy of the photon, and σ_{abs} is the absorption cross section of the NP at the excitation wavelength.[4]

We assume a Gaussian diffraction limited laser beam with diameter d and calculate

$$d = \frac{1.22\lambda}{NA}$$ where λ is the wavelength of the laser (485nm) and NA is the numerical aperture (1.4) of the objective, yielding r = 211 nm.

The value of σ_{abs} is obtained by multiplying the value of the extinction coefficient at the absorption maximum (estimated to be ~6 x 10^5 $M^{-1}cm^{-1}$ from Ref. 3 by 0.6 to account for the wavelength of excitation (485 nm). This yields a value for σ_{abs} of ~1.4 x 10^{-15} cm^2 after units conversion.

The power at the sample was calculated by multiplying the value measured before the beam enters the microscope by 0.10 which is the factor by which the beam is attenuated by the time it reaches the sample. For this calculation, we chose the lowest laser power at which the red emission (~650 nm) could be measured (100μW) to yield P=10μW or 7kW/cm^2. The value of Γ was 10MHz. Plugging these values into the above equation for <N> gives a value of 1.7. This is likely an overestimate given that the emission signal from the CT state is clearly still linear at this power (ESI Figure S4(c)).

One likely source of uncertainty in the calculation of <N> is the value of σ_{abs}. Another route to estimate the extinction coefficient is to extract the radiative lifetime from the emission lifetime (τ) and the quantum yield (φ). These quantities are 3ns and 0.9, respectively. Using the relation

$\varphi = \frac{\tau}{\tau_0}$ where the subscript denotes the radiative lifetime, this quantity is calculated to be 3.3ns. Next, the following approximate expression, given in Ref. 5, can be used to estimate the maximum extinction coefficient (ϵ_{max}) given τ_0 in seconds, the energy at the peak of the absorption band (ν) and the FWHM of the absorption band (Δν), both in cm^{-1}

$$\epsilon_{max} = (3 \times 10^{-9} \nu^2 \Delta\nu \tau_0)^{-1}$$

From Figure 1 of Ref. 2, we estimate the peak of the absorption band to be 510nm (19608cm^{-1}) and the FWHM to be 1540cm^{-1}. These values give an ϵ_{max} of ~2x10^5 M^{-1}cm^{-1} or an σ_{abs} of ~4 x 10^{-16} cm^2 after multiplying by 0.6 as above. Using this value to estimate <N> at 7kW/cm^2 gives 0.5.

The probability distribution $P_{<N>}(n)$ per pulse corresponding to a single excitation (n=1) or a bi-exciton (n=2) is given by

$$P_{<N>}(n) = e^{-<N>} \frac{<N>^n}{n!}$$

For <N> = 0.5, this gives 30% probability for n=1 and 8% probability for n=2. Therefore, bi-excitons are expected to be formed at ~27% of the efficiency of single excitons for an excitation power density of 7kW/cm^2. This may account for the value of $g^{(2)}(0)$ of 0.2 obtained for the main emission peak. However, it is much smaller than the value of 0.8 measured for $g^{(2)}(0)$ at 650nm suggesting that this band does not arise from excitation of two CT transitions on the SiNPs.

References:

(1) Tcherniak, A.; Reznik, C.; Link, S.; Landes, C. F. Fluorescence Correlation Spectroscopy: Criteria for Analysis in Complex Systems. *Analytical Chemistry* **2009**, *81*, 746–754.

(2) Lin, H.; Hania, R. P.; Bloem, R.; Mirzov, O.; Thomsson, D.; Scheblykin, I. G. Single Chain versus Single Aggregate Spectroscopy of Conjugated Polymers. Where Is the Border? *Physical Chemistry Chemical Physics* **2010**, *12*, 11770.

(3) Li, Q.; Luo, T.-Y.; Zhou, M.; Abroshan, H.; Huang, J.; Kim, H. J.; Rosi, N. L.; Shao, Z.; Jin, R. Silicon Nanoparticles with Surface Nitrogen: 90% Quantum Yield with Narrow Luminescence Bandwidth and the Ligand Structure Based Energy Law. *ACS Nano* **2016**, *10*, 8385–8393.

(4) Smyder, J. A.; Amori, A. R.; Odoi, M. Y.; Stern, H. A.; Peterson, J. J.; Krauss, T. D., *Phys. Chem. Chem. Phys.*, **2014**, *16*, 25723–25728

(5) N. J. Turro, *Modern Molecular Photochemistry*, University Science Books, 1991